

COMMUNICATION

A Molecular Aluminium Fulleride

Samuel Ray Lawrence,^{a,b} Tobias Rüffer,^b Andreas Stasch,^{a*} and Robert Kretschmer^{b*},Received 00th January 20xx,
Accepted 00th January 20xx

DOI: 10.1039/x0xx00000x

The reaction of alumylene [(^{Dipp}nacnac)Al] (1) with C₆₀ fashions the first example of a structurally characterised aluminium-fulleride complex, [(^{Dipp}nacnac)Al]₃C₆₀ (2), in which the Al centres are covalently bound to significantly elongated 6:6 bonds. Hydrolysis of 2 yields C₆₀H₆ and the reaction of 2 with [(^{Me}s⁺nacnac)Mg]₂ cleaved the Al fragments by affording the fulleride [(^{Me}s⁺nacnac)Mg]₆C₆₀.

Buckminsterfullerene, C₆₀, has solidified a foothold across all disciplines of physical science, owing to the diverse range of electronic and physical properties that this carbon allotrope exhibits.¹ Soon after the discovery of a multi-gram preparation of C₆₀,² there was immediate curiosity in the intercalation of alkali-metals into the lattice of C₆₀ to give films of A_nC₆₀ stoichiometries (A = alkali metal, n = 1–12),³ with much of that interest being directed towards the study of the superconducting A₃C₆₀ (A = K, Rb) phase.⁴ Doping of C₆₀ was further extended to the alkaline-earth metals, which afford assemblies of varying Ae_nC₆₀ stoichiometry (Ae = alkaline-earth metal, n = 1–6),⁵ and the area still remains a hot topic today.⁶ Furthermore, the facile reduction of C₆₀ with magnesium(I) reagents has afforded well-defined ionic fulleride complexes that promise further reactivity with reactive low-valent main-group compounds.⁷ Despite this, and with the exception of carbon, less regard has been afforded to the interaction between p-block elements and fullerenes. Covalent functionalisation of a fullerene cage is typically carried out through the nucleophilic attack of base-generated carbanions, known as the Bingel Reaction, with one or two carbon atoms adding across a 6:6 bond of “double bond” character, and [4+2] as well as [3+2] cycloadditions at these positions are also common.⁸ Electronically destabilised carbenes, generated *in-situ* likewise add in this fashion (Figure 1a)⁹ as do low-valent silicon and germanium surrogates under photolytic or high temperature conditions.¹⁰

In contrast, the reaction of the *N*-heterocyclic carbene IDipp (1,3-bis(2,6-diisopropylphenyl)imidazol-2-ylidene) with C₆₀ produces a zwitterionic compound with the negative charge delocalised across the C₆₀ cage and a single C–C bond between the carbene and the fullerene (Figure 1a).¹¹

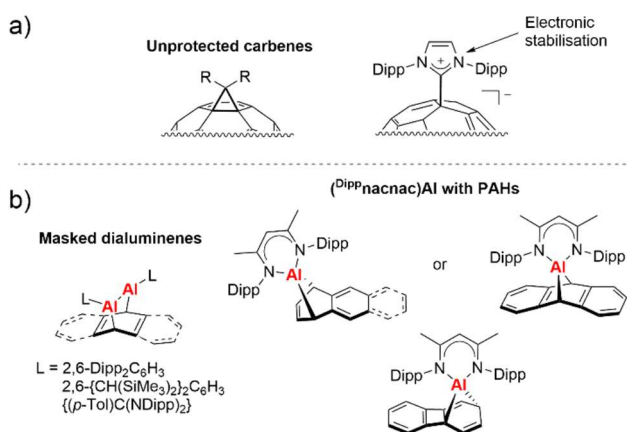


Figure 1: a) Different binding modes of carbenes to C₆₀; b) Examples of 1,4-additions of aluminium(I) compounds to arenes and polyaromatic hydrocarbons; Dipp = 2,6-*i*-Pr₂C₆H₃.

In recent years, reports of NHC analogues of Group 13 and Group 14 elements in low oxidation states have been forthcoming at a rapid pace.¹² Of these compounds, [(^{Dipp}nacnac)Al] **1**^{13a,b} (^{Dipp}nacnac = HC{CH₃CN(Dipp)}₂, Dipp = 2,6-*i*-Pr₂C₆H₃) is among those best explored for transition-metal-like activations.^{13c} The direct addition of **1**,¹⁵ but also those of “masked dialuminenes”,¹⁴ to arenes and extended π-systems afford predominantly 1,4-addition products that have very recently been reported (Figure 1b). Given that only a small number of examples of aluminium-fullerene mixtures exist, primarily as nanocomposites,¹⁶ we investigated the reactivity of the aluminium NHC analogue **1** with C₆₀, and our findings are reported herein.

^aEaStCHEM School of Chemistry, University of St Andrews, North Haugh, St Andrews, KY16 9ST, UK. E-mail: as411@st-andrews.ac.uk

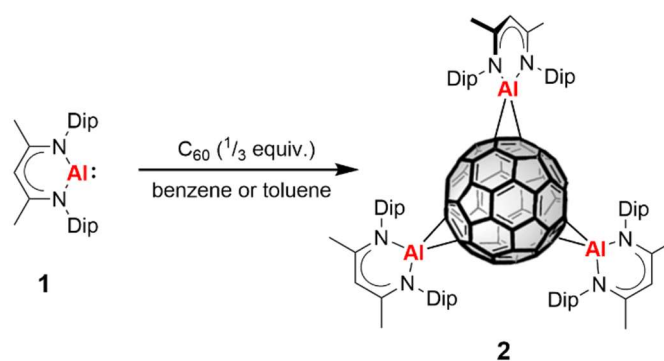
^bInstitute of Chemistry, Chemnitz University of Technology, 09111 Chemnitz, Germany. E-mail: robert.kretschmer@chemie.uni-jena.de

† Electronic supplementary information (ESI) available: Experimental, spectroscopic, crystallographic (CCDC 2253113), and computational details (PDF).

Reaction of **1** with a third of an equivalent of C_{60} at room temperature in benzene or toluene immediately results in a dark green solution and full consumption of **1** is observed by 1H NMR spectroscopy after one day at room temperature; see the ESI for details on the impact of the stoichiometry. Deep red single-crystals suitable for an X-ray diffraction analysis deposit from a toluene- d_8 solution after a further two days (Scheme 1).

$[(^{Dipp}nacnac)Al]_3C_{60}$ **2** crystallised in the space group $C2/c$, with half a molecule in the asymmetric unit (Figure 2a), and possesses crystallographically imposed C_2 symmetry, and pseudo C_3 symmetry (Figure 2b,c). Chirality arises from the helical nature of the three $[(^{Dipp}nacnac)Al]$ groups surrounding C_{60} (see Figure S24), but due to the centrosymmetric space group both enantiomers are present in the unit cell. The arrangement of the three $[(^{Dipp}nacnac)Al]$ units around the C_{60} cage are reminiscent of the major isomer of $C_{60}H_6$ (1,2,33,41,42,50- $C_{60}H_6$).¹⁷ The aluminium centres coordinate to C_{60} at 6:6 bonds, forming AlC_2 metallacyclopropane moieties, much in the same manner as unprotected carbenes (see Figure 1a). Such $(^{Dipp}nacnac)AlC_2$ metallacycle motifs are known, arising from the reaction of **1** with terminal and strained alkenes.¹⁸ The Al–C bond lengths in **2** agree with those structures, albeit with significant elongation (1.9779(2), 1.9701(2), and 1.9551(3) Å in **2** vs 1.940(4) and 1.948(3) Å in $[(^{Dipp}nacnac)Al(\eta^2\text{-norbornane})]$, for example).^{18a}

The 1H NMR spectrum of **2** shows characteristic resonances of a $^{Dipp}nacnac$ ligand. These are singlets at 4.99 ppm (γ -CH) and 1.66 ppm (backbone- CH_3), four doublets (1.07, 1.08, 1.38 and 1.44 ppm), and two septets (3.53 and 3.63 ppm) for the iPr hydrogens corroborating the slightly asymmetric environments of the halves of the $[(^{Dipp}nacnac)Al]$ units (see Figure S26). The



Scheme 1: Synthesis of aluminium fulleride **2**.

$^{13}C\{^1H\}$ NMR spectrum of **2** supports the structure and symmetry shown in Figure 2a, with one sp^3 -C resonance at 76.3 ppm and nine sharp C_{60} resonances between 137.8–172.2 ppm of similar intensities. The sp^3 -C resonance is in the same region as in the related structure $[(^{Dipp})_2Si]C_{60}$ (71.1 ppm).^{10a} Overall, this assignment mirrors that of $C_{60}H_6$ (one sp^3 -C at 52.3 ppm and nine sp^2 -C between 140–160 ppm)¹⁷ and suggests both a 3-fold symmetry axis and three 2-fold symmetry axes in solution, as indicated (Figure 2b,c). All remaining ^{13}C NMR resonances in the spectrum correspond to the $^{Dipp}nacnac$ -ligand environments, as confirmed by 2D NMR spectroscopic assignments.

As activations of alkenes and arenes by **1** are known to be reversible at elevated temperatures,^{15,18} complex **2** was studied at 80 °C in deuterated toluene. The 1H NMR spectrum confirmed that the symmetry in solution remained unchanged and resonances were not significantly shifted compared with those

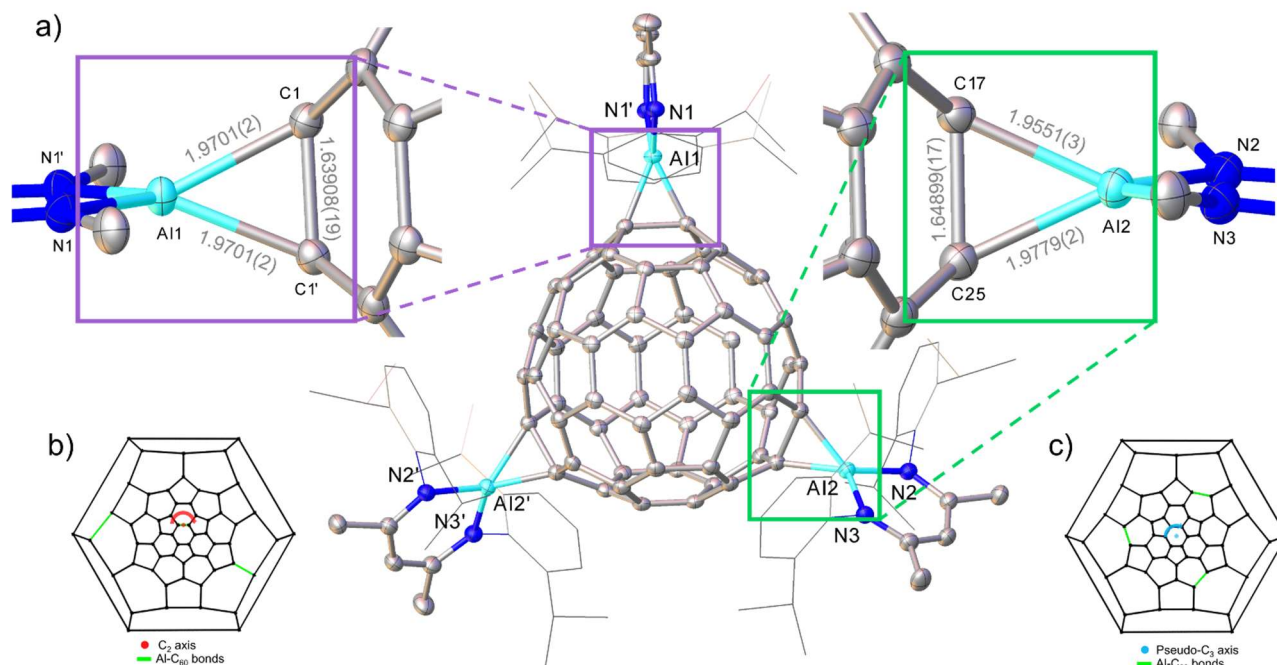


Figure 2: a) Molecular structure of **2** (symmetry transformations used to generate equivalents atoms marked with ' : 1-x, y, 3/2-z); 50% thermal ellipsoids, solvent molecules and H atoms omitted and *N*-2,6-diisopropylphenyl groups shown as wireframe for clarity, bond length values given in Å); b) and c) Schlegel diagrams looking down the C_2 and pseudo- C_3 axis, respectively.

obtained in experiments at room temperature. Heating was, however, accompanied by significant decomposition of **2** followed by a colour change to brown, and more complete decomposition with the formation of an intractable mixture of products. Reagents chosen to trap the possible reversible production of $[(\text{Dippnacnac})\text{Al}]$ **1** from **2** at high temperatures, instead displayed unique reactivities with **2** in the form of intractable mixtures of products (for more information, see ESI).

Inspection of the Dippnacnac ligand-aluminium distances in **2** reveals significantly contracted contacts (average Al–N bond length: 1.8673(18) Å) compared to those in **1** (1.957(2) Å).^{13a} This close association affects a concomitant widening of the N–Al–N bond angle to accommodate the steric bulk of the Dipp groups (average N–Al–N bond angle: 99.6(1)° in **2** vs 89.86(8)° in **1**),^{13a} and both properties signify a larger point charge on the aluminium centre, i.e., oxidation to Al^{3+} . The overall spherical shape of C_{60} is not significantly changed outside the localisation of aluminium coordination (average radius of the [60]fullerene in **2** excluding Al–C₂ carbon atoms: 3.543 Å; compared with neutral C_{60} 3.525 Å,¹ and $[(\text{LMg})_6\text{C}_{60}]$ structures 3.554–3.559 Å).^{7a} Likewise, the average C–C(C_{60}) bond lengths in **2** (excluding Al–C₂) compare well with those of neutral C_{60} (6:6 1.396(3) Å, 6:5 1.445(3) Å, overall 1.429(3) Å; vs 6:6 1.394 Å, 6:5 1.448 Å, overall 1.43 Å in neutral C_{60}).¹⁹ In contrast, the cage-radii for carbon atoms directly bound to aluminium average to 3.836 Å and other C(C_{60}) atoms at larger distances from the centre are amongst those adjacent to the Al–C₂ motifs. Furthermore, C–C bond lengths bridging the aluminium centres are significantly lengthened to 1.639(4) and 1.649(3) Å. This presents a situation in which aluminatation of [60]fullerene pulls the immediate carbon atoms out from the cage, with significant pyramidalization of the affected C atoms, as is observed in $[(\text{LMg})_2\text{C}_{60}]$ compounds.^{7a}

A UV/Vis spectroscopic analysis of **2** in toluene (see Figures S9–10), reveals maxima in the visible region at 426 and 632 nm in addition to a maximum in the UV regime (341 nm, $\epsilon \approx 68000 \text{ mol}^{-1} \text{ dm}^3 \text{ cm}^{-1}$).

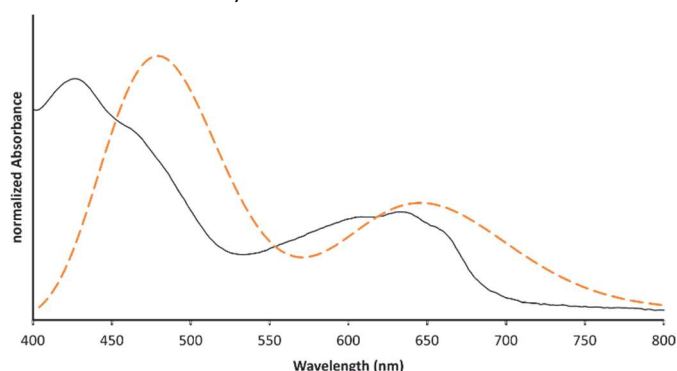
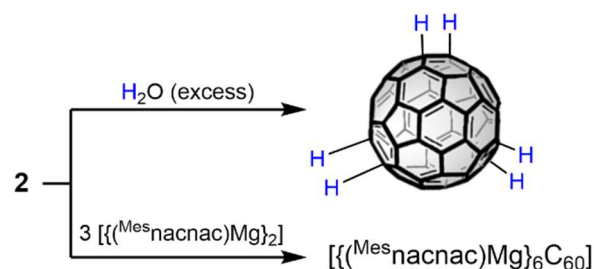


Figure 3: Experimental (black) and simulated (orange-dashed) UV/Vis spectrum of **2**. The simulated spectrum was calculated from time-dependent DFT at the B3LYP10 level of theory. See the ESI for details.

The molecular orbitals of **2** have been calculated at the B3LYP10(GD3BJ)/6-31G(d,p)/(SMD(toluen)) level of theory²⁰ (Figures S27–29). Both the doubly degenerate HOMO and the

HOMO-1 originate from a constructive interaction of the s-type lone pairs of the three $[(\text{Dippnacnac})\text{Al}]$ units, i.e., the respective HOMO, and the former C_{60} LUMO level by overall six electrons. This and concomitant interaction of C_{60} π^* orbitals with the out-of-plane p-type orbitals at aluminium contribute to the significant C–C bond lengthening. The triply degenerate LUMO is entirely centred on the nacnac framework and C_{60} contributes to both the LUMO+1 and the doubly degenerate LUMO+2. Time-dependent DFT calculations were performed to assign the observed absorption events in the visible region. Although slightly red-shifted, the experimental and the simulated spectrum are in good agreement, Figure 3. The experimentally observed absorption at 632 nm is associated with transitions from the doubly-degenerated HOMO to the doubly-degenerated LUMO+2 calculated to occur at 647 nm. The absorptions at shorter wavelength, i.e. 426 nm, originates mainly from transitions from the HOMO-1 to the LUMO+2 and are calculated to occur at 489 nm.



Scheme 2: Further reactivity of **2** with H_2O and $[(\text{Mesnacnac})\text{Mg}]_2$

The regioselectivity of the aluminium binding to the cage presents a rare opportunity for selective functionalisation at these positions. In this vein, a toluene solution of **2** was quenched with water under an inert atmosphere. The ^1H NMR spectrum of the crude reaction mixture shows a dominant singlet at 5.18 ppm (in toluene- d_8), corresponding to 1,2,33,41,42,50- C_{60}H_6 ¹⁷ and resonances referring to DippnacnacH (Scheme 2) evidencing the selectivity of the protocol. Next, compound **2** was treated with $[(\text{Mesnacnac})\text{Mg}]_2$ (Mes = 2,4,6- $\text{Me}_3\text{C}_6\text{H}_2$) as a reductant,²¹ causing a retro-Bingel reaction²² (Scheme 2). To our surprise, not only were the $[(\text{Dippnacnac})\text{Al}]$ units removed from the sphere, but they were also replaced with $[(\text{Mesnacnac})\text{Mg}]$ groups, culminating in the formation of $[(\text{Mesnacnac})\text{Mg}]_6\text{C}_{60}$ as the main product, as confirmed by ^1H and $^{13}\text{C}\{^1\text{H}\}$ NMR spectroscopy.^{7a}

In summary, we report the facile synthesis of a tri-substituted aluminium fulleride, $[(\text{Dippnacnac})\text{Al}]_3\text{C}_{60}$ **2**, which was characterised by ^1H and ^{13}C NMR spectroscopy, X-ray crystallography, DFT computational studies, and further methods. The regioselective covalent binding of the $[(\text{Dippnacnac})\text{Al}]$ units to the C_{60} cage could be exploited chemically and the hydrolysis of **2** occurred, selectively affording C_{60}H_6 . Reduction of **2** using a magnesium(I) complex removed all $[(\text{Dippnacnac})\text{Al}]$ moieties in a retro-Bingel-type reaction giving rise to the fulleride $[(\text{Mesnacnac})\text{Mg}]_6\text{C}_{60}$.

The work is dedicated to Thomas Weiske and Helmut Schwarz for their seminal work on He@C₆₀²³ and on the occasion of their 65th and 80th birthday, respectively. The project was financially supported by the Deutsche Forschungsgemeinschaft (DFG, KR4782/3-1), the EPSRC (PhD studentship for SRL; EP/N509759/1), and the Chemnitz University of Technology. We thank the Rechenzentrum of the Friedrich Schiller University Jena for the allocation of computer time.

Author Contributions

SRL performed the synthesis and characterisation of the new compounds reported. SRL, AS and RK conceptualised the study and finalised the manuscript for submission. RK performed the computational analysis and TR finalised the X-ray diffraction analysis of **2** for publication.

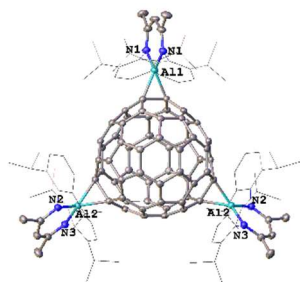
Conflicts of interest

There are no conflicts to declare.

Notes and references

- 1) a) *Fullerenes: Principles and Applications*, ed. F. Langa De La Puente and J. -F. Nierengarten, Royal Society of Chemistry, London, 2nd edn., 2011; b) *Fullerenes - Chemistry and Reactions*, ed. A. Hirsch and M. Brettreich, Wiley-VCH, Weinheim, 2005.
- 2) W. Krätschmer, L. D. Lamb, K. Fostiropoulos and D. R. Huffman, *Nature*, 1990, **347**, 354–358.
- 3) a) C. A. Reed and R. D. Bolskar, *Chem. Rev.*, 2000, **100**, 1075–1120.
- 4) M. J. Rosseinsky, *Chem. Mater.*, 1998, **10**, 2665–2685.
- 5) a) R. C. Haddon, G. P. Kochanski, A. F. Hebard, A. T. Flory and R. C. Morris, *Science*, 1992, **258**, 1636–1638; b) G. K. Wertheim, D. N. E. Buchanan and J. E. Rowe, *Science*, 1992, **258**, 1638–1640.
- 6) a) L. Hou, X. Cui, B. Guan, S. Wang, R. Li, Y. Liu, D. Zhu and J. Zheng, *Nature*, 2022, **606**, 507–510; b) E. Meirzadeh, A. M. Evans, M. Rezaee, M. Milich, C. J. Dionne, T. P. Darlington, S. T. Bao, A. K. Bartholomew, T. Handa, D. J. Rizzo, R. A. Wiscons, M. Reza, A. Zangiabadi, N. Fardian-Melamed, A. C. Crowther, P. J. Schuck, D. N. Basov, X. Zhu, A. Giri, P. E. Hopkins, P. Kim, M. L. Steigerwald, J. Yang, C. Nuckolls and X. Roy, *Nature*, 2023, **613**, 71–76.
- 7) a) S. R. Lawrence, C. A. Ohlin, D. B. Cordes, A. M. Z. Slawin and A. Stasch, *Chem. Sci.*, 2019, **10**, 10755–10764; b) S. R. Lawrence, D. B. Cordes, A. M. Z. Slawin and A. Stasch, *Dalton Trans.*, 2019, **48**, 16936–16942.
- 8) R. Caballero, P. de la Cruz and F. Langa, in *Fullerenes: Principles and Applications*, ed. F. Langa De La Puente and J.-F. Nierengarten, Royal Society of Chemistry, London, 2nd edn., 2011, ch. 3, pp. 66–124.
- 9) a) M. Yamada, T. Akasaka and S. Nagase, *Chem. Rev.*, 2013, **113**, 7209–7264; b) H. Nikawa, T. Nakahodo, T. Tsuchiya, T. Wakahara, G. M. A. Rahman, T. Akasaka, Y. Maeda, M. T. H. Liu, A. Meguro, S. Kyushin, H. Matsumoto, N. Mizorogi and Shigeru Nagase, *Angew. Chem. Int. Ed.*, 2005, **44**, 7567–7570.
- 10) a) T. Akasaka and W. Ando, *J. Am. Chem. Soc.*, 1993, **115**, 1605–1606; b) T. Kusakawa, A. Shike and W. Ando, *Tetrahedron*, 1996, **52**, 4995–5005; c) M. Kako, D. Inaba, K. Minami, R. Iida, T. Nakahodo and T. Akasaka, *Heteroatom Chem.*, 2014, **25**, 584–591.
- 11) H. Li, C. Risko, J. H. Seo, C. Campbell, G. Wu, J.-L. Brédas and G. C. Bazan, *J. Am. Chem. Soc.*, 2011, **133**, 12410–12413.
- 12) M. Asay, C. Jones and Matthias Driess, *Chem. Rev.*, 2011, **111**, 354–396.
- 13) a) C. Cui, H. W. Roesky, H.-G. Schmidt, M. Noltemeyer, H. Hao and F. Cimpoesu, *Angew. Chem. Int. Ed.*, 2000, **39**, 4274–4276; b) O. Kysliak, H. Görls and R. Kretschmer, *Dalton Trans.*, 2020, **49**, 6377–6383; c) Y. Liu, X. Ma, Z. Yang and H. W. Roesky, *Coord. Chem. Rev.*, 2018, **374**, 387–415.
- 14) a) R. J. Wright, A. D. Phillips and P. P. Power, *J. Am. Chem. Soc.*, 2003, **125**, 10784–10785; b) T. Agou, K. Nagata, and N. Tokitoh, *Angew. Chem. Int. Ed.*, 2013, **52**, 10818–10821; c) C. Bakewell, K. Hobson and C. J. Carmalt, *Angew. Chem. Int. Ed.*, 2022, **61**, e202205901.
- 15) a) C. Bakewell, M. Garçon, R. Y. Kong, L. O'Hare, A. J. P. White and M. R. Crimmin, *Inorg. Chem.*, 2020, **59**, 4608–4616; b) R. Y. Kong and M. R. Crimmin, *J. Am. Chem. Soc.*, 2020, **142**, 11967–11971; c) R. Y. Kong and M. R. Crimmin, *Angew. Chem. Int. Ed.*, 2021, **60**, 2619–2623; d) A. Dmitrienko, M. Pilkington and G. I. Nikonov, *Mendeleev Commun.*, 2022, **32**, 68–70.
- 16) a) D. W. Owens, C. M. Aldao, D. M. Poirier and J. H. Weaver, *Phys. Rev. B*, 1995, **51**, 17068–17072; b) M. L. Wang, Q. L. Song, H. R. Wu, B. F. Ding, X. D. Gao, X. Y. Sun, X. M. Ding and X. Y. Hou, *Organic Electronics*, 2007, **8**, 445–449.
- 17) M. S. Meier, B. R. Weedon and H. P. Spielmann, *J. Am. Chem. Soc.*, 1996, **118**, 11682–11683.
- 18) a) C. Bakewell, A. J. P. White and M. R. Crimmin, *Angew. Chem. Int. Ed.*, 2018, **57**, 6638–6642; b) C. Bakewell, A. J. P. White and M. R. Crimmin, *Chem. Sci.*, 2019, **10**, 2452–2458.
- 19) W. I. F. David, R. M. Ibberson, J. C. Matthewman, K. Prassides, T. J. S. Dennis, J. P. Hare, H. W. Kroto, R. Taylor and D. R. M. Walton, *Nature*, 1991, **353**, 147–149.
- 20) See the ESI for details on the computational protocol. The B3LYP10 functional has previously been identified to provide an unambiguous description of structural and of electronic ground state properties of a dinuclear aluminium complex: F. L. Portwich, Y. Carstensen, A. Dasgupta, S. Kupfer, R. Wyrwa, H. Görls, C. Eggeling, B. Dietzek, S. Grafe, M. Wachtler, and R. Kretschmer, *Angew. Chem., Int. Ed.* 2022, **61**, e202117499.
- 21) a) C. Jones, *Nat. Rev. Chem.*, 2017, **1**, 0059; b) S. J. Bonyhady, C. Jones, S. Nembenna, A. Stasch, A. J. Edwards and G. J. McIntyre, *Chem. Eur. J.*, 2010, **16**, 938–955.
- 22) a) M. A. Herranz, F. Diederich and L. Echegoyen, *Eur. J. Org. Chem.*, 2004, 2299–2316; b) N. N. P. Moonen, C. Thilgen, L. Echegoyen and F. Diederich, *Chem. Commun.*, 2000, 335–336.
- 23) T. Weiske, D. K. Böhme, J. Hrušák, W. Krätschmer and H. Schwarz, *Angew. Chem. Int. Ed. Engl.*, 1991, **30**, 844–886.

Table of Contents Graphic



Go-Al! Low Valent Aluminium Scores a Hat-trick by converting C_{60} to a tri-substituted molecular aluminium fulleride.